p52Shc regulates the sustainability of ERK activation in a RAF-independent manner

Ryo Yoshizawa[a,b], Nobuhisa Umeki[a], Akihiro Yamamoto[a], Mariko Okada[c,d], Masayuki Murata[b], and Yasushi Sako[a,*]

[a]Cellular Informatics Lab, RIKEN, Wako, Saitama 351-0198, Japan; [b]Department of Life Sciences, Graduate School of Arts and Sciences, The University of Tokyo, Komaba, Meguro, Tokyo 153-8902, Japan; [c]Institute for Protein Research, Osaka University, Suita, Osaka 565-0871, Japan; [d]Center for Drug Design and Research, National Institutes of Biomedical Innovation, Health and Nutrition, Ibaraki 567-0085, Japan

ABSTRACT **p52SHC (SHC) and GRB2 are adaptor proteins involved in the RAS/MAPK (ERK) pathway mediating signals from cell-surface receptors to various cytoplasmic proteins. To further examine their roles in signal transduction, we studied the translocation of fluorescently labeled SHC and GRB2 to the cell surface, caused by the activation of ERBB receptors by heregulin (HRG). We simultaneously evaluated activated ERK translocation to the nucleus. Unexpectedly, the translocation dynamics of SHC were sustained when those of GRB2 were transient. The sustained localization of SHC positively correlated with the sustained nuclear localization of ERK, which became more transient after SHC knockdown. SHC-mediated PI3K activation was required to maintain the sustainability of the ERK translocation regulating MEK but not RAF. In cells overexpressing ERBB1, SHC translocation became transient, and the HRG-induced cell fate shifted from a differentiation to a proliferation bias. Our results indicate that SHC and GRB2 functions are not redundant but that SHC plays the critical role in the temporal regulation of ERK activation.**

Monitoring Editor
Jorge Torres
University of California, Los Angeles

Received: Jan 8, 2021
Revised: Jun 22, 2021
Accepted: Jul 8, 2021

INTRODUCTION

Numerous types of cell-surface receptors function with adaptor proteins to facilitate the transmission and amplification of extracellular signals into the cytoplasm, where they stimulate various cell responses. One of the receptor tyrosine kinase (RTK) families, ERBB (ERBB1–4), belongs to such cell-surface receptors. ERBB family members are activated by various growth factors and interact with adaptor proteins, including p52SHC and GRB2, to propagate growth factor signaling to the RAS/MAPK (extracellular signal–regulated kinase; ERK) and PI3K/AKT (PKB) pathways that regulate cell proliferation, differentiation, apoptosis, and metabolism (Mendoza *et al.*, 2011; Nepstad *et al.*, 2020).

p52SHC (hereafter referred to as SHC) is one of three isoforms of a family of proteins (p46, p52, and p66) that plays important roles in both normal and oncogenic cell signaling and is associated with a poor prognosis in breast cancer patients (Gu *et al.*, 2000; Davol *et al.*, 2003). SHC and its isoforms contain an amino-terminal phosphotyrosine-binding (PTB) domain, a central region of the collagen homology 1 (CH1) domain, and a carboxy-terminal Src homology 2 (SH2) domain (Pelicci *et al.*, 1992). The PTB domain enables the translocation of SHC to the plasma membrane, where it recognizes the phosphorylated NXXY motif of the ERBB receptors. Once associated with an ERBB receptor, SHC is phosphorylated at $Tyr^{239/240}$ and Tyr^{317}. These phosphotyrosine residues interact with SH2 domain–containing proteins including GRB2, resulting in the activation of multiple signaling pathways (Ravichandran, 2001). For example, an increase in the density of the GRB2-SOS complex on the plasma membrane through the interaction between phosphorylated SHC and GRB2 contributes to signal amplification from ERBB receptors to RAS. It has been reported also that SHC is required for the full activation of RAS/MAPK signaling when cells are stimulated with growth factors at a low concentration (Lai and Pawson, 2000). In

This article was published online ahead of print in MBoC in Press (http://www.molbiolcell.org/cgi/doi/10.1091/mbc.E21-01-0007) on July 14, 2021.

Competing interests: The authors declare no competing financial or other interests in relation to this study.

Author contributions: Conceived and designed the experiments: R.Y., N.U., M.M., M.O., and Y.S. Performed the experiments: R.Y. and A.Y. Analyzed the data: R.Y. Wrote the paper: R.Y. and Y.S.

*Address correspondence to: Yasushi Sako (sako@riken.jp).

Abbreviations used: B1MCF7, EGFR-overexpressing MCF7 cells; HRG, heregulin; SHC, p52SHC.

addition, SHC interacts with the complex of 14-3-3 and PI3K for activation of the RAS/MAPK and PI3K/AKT signaling pathways (Ursini-Siegel *et al.*, 2012; Suen *et al.*, 2018).

Another adaptor protein, GRB2, contains an SH2 domain that recognizes the pYXN motif of upstream proteins, including the ERBBs, and two SH3 domains that bind to the proline-rich motif in downstream effector proteins (Songyang *et al.*, 1994; Sparks *et al.*, 1996). The translocation of GRB2 to the plasma membrane, where it interacts with phosphorylated ERBBs and SHC, results in the recruitment of effector proteins, including SOS1- and GRB2-associated binder 1 (GAB1), to the plasma membrane and activation of the RAS/MAPK and PI3K/AKT signaling pathways (Pawson, 2007; Bisson *et al.*, 2011). Thus, the recruitments of GRB2 and SHC to the plasma membrane upon receptor activation have been thought to be biologically redundant processes for the promotion of RAS/MAPK and PI3K/AKT signaling pathways (Saucier *et al.*, 2002, 2004; Oku *et al.*, 2012), even though there is a stronger activation of DNA synthesis under SHC than GRB2 (Oku *et al.*, 2012).

It is widely accepted that in the RAS/MAPK signaling pathway, differences in the duration of ERK activation correlate with distinct cellular responses, that is, proliferation or differentiation (Marshall, 1995). ERK is translocated to the nucleus and regulates the activation of nuclear transcription factors (Brunet *et al.*, 1999; Bouchard *et al.*, 2004; Caunt and McArdle, 2012). In MCF7 and PC12 cells, the transient activation of ERK by the epidermal growth factor (EGF) leads to cell proliferation, while the sustained activation of ERK by heregulin (HRG) or nerve growth factor (NGF) leads to cell differentiation (Marshall, 1995; Kao *et al.*, 2001; Nagashima *et al.*, 2007). Various mechanisms have been suggested for the regulation of the activation dynamics of ERK, including growth factor–dependent regulation (Birtwistle *et al.*, 2007), positive and negative feedback loops in the RAF-MEK-ERK pathway (Santos *et al.*, 2007; Avraham and Yarden, 2011), cross-talk between the RAS/MAPK and PI3K/AKT pathways (Egan *et al.*, 1993; Kiyatkin *et al.*, 2006), and RAS- and RAP-dependent regulation (Kao *et al.*, 2001; Sasagawa *et al.*, 2005; Nakakuki *et al.*, 2008). To our knowledge, however, the roles of SHC and GRB2 in the regulation of ERK activation dynamics and the determination of cell fate have not been discussed or reported in any great depth.

In our present study, we aimed to better understand the functions of SHC and GRB2 during the signal transduction dynamics of ERK and their further roles in the determination of cell fates. In the analyses, we observed the translocation dynamics of SHC, GRB2, and ERK after HRG stimulation using multimode, dual-color fluorescence microscopy in living MCF7 cells. We then analyzed the translocation dynamics of these proteins and from our findings suggest a novel role of SHC in HRG signaling and subsequent cell fate decisions.

RESULTS

The distinct translocation dynamics of SHC and GRB2 upon HRG stimulation

To investigate the spatiotemporal features of the SHC and GRB2 responses to HRG stimulation, we first observed their translocation dynamics to the plasma membrane from the cytoplasm in living MCF7 cells after stimulation with HRG. For the visualization of these proteins in the cells, Halo protein and GFP were fused to the N-terminus of SHC and GRB2, respectively (hereafter referred to as Halo-SHC and GFP-GRB2) (Supplemental Figure S1). The expression of these proteins was confirmed by SDS–PAGE analysis. The apparent molecular masses of the Halo-SHC and GFP-GRB2 proteins were determined by Western blotting analysis as 86 and 52 kDa, respectively (Supplemental Figure S1A), consistent with their expected molecular sizes. The relative expression levels of the transfected Halo-SHC and GFP-GRB2 were about 50% or less of those of the endogenous molecules and did not affect the endogenous expression (Supplemental Figure S1, C and D). We anticipated that the lower expression of the tagged molecules would allow us to analyze the translocation dynamics of SHC and GRB2 without changing the intrinsic properties of these proteins.

Halo-SHC and GFP-GRB2 were observed on the cytoplasmic surface of the plasma membrane using total internal reflection fluorescence microscopy (TIRFM) (Figure 1A). In our experiment, Halo protein was conjugated with tetramethylrhodamine (TMR). Both adaptor proteins were found to be mainly distributed in the cytoplasm (Supplemental Figure S2) and circulate between the cytoplasm and the plasma membrane before and after HRG stimulation. Application of HRG to the culture medium increased the densities of both proteins on the cell surface, and the increased membrane localization of Halo-SHC was sustained for at least 60 min after HRG stimulation (Figure 1B), whereas that of GFP-GRB2 was transient (Figure 1C). In subsequent confocal microscopy observations, no association with the endosomal membrane was evident for either GFP-GRB2 or Halo-SHC, even after HRG stimulation of the cells (Supplemental Figure S2A).

It is generally thought that GRB2 translocation to the plasma membrane after growth factor stimulation is caused through its association with phosphorylated ERBBs and phosphorylated SHC, which is itself bound to phosphorylated ERBBs. Western blotting analysis under the same conditions as used for cell imaging revealed that phosphorylation of the GRB2-binding site on SHC ($pTyr^{317}$) was increased after HRG stimulation and persisted for as long as the translocation of Halo-SHC (Supplemental Figure S3C). In addition, the major SHC- and GRB2-binding sites of all four ERBBs (ERBB1–B4) were persistently phosphorylated over a 60 min period without significant differences between the phosphorylation levels of the SHC- and GRB2-binding sites (Supplemental Figure S3C). These results indicated that SHC and GRB2 have distinct translocation dynamics in MCF7 cells that are stimulated by HRG via previously unknown mechanisms.

The sustained localization of SHC at the plasma membrane correlates with the sustained activation of ERK

We next observed the translocation dynamics of GFP-tagged ERK2 (GFP-ERK) from the cytoplasm to the nucleus after HRG stimulation of the cells. The apparent molecular mass of the GFP-ERK determined from Western blotting analysis was 72 kDa (Supplemental Figure S1B), consistent with the expected molecular size. Previous reports have reported that HRG induces a sustained activation of ERK in MCF7 cells, which leads to cell differentiation (Marshall, 1995; Kao *et al.*, 2001; Nagashima *et al.*, 2007). We confirmed here that EGF and HRG induced transient and sustained translocation of ERK to the nucleus, respectively (Supplemental Figure S4), that is, the probe used in this study allowed us to detect the translocation dynamics of ERK in MCF7 cells. GFP-ERK was found to be persistently translocated to the nucleus and persistently phosphorylated up to at least 60 min after HRG stimulation (Figure 1, A and D; Supplemental Figure S3C).

To evaluate the possible correlation between SHC and GRB2 dynamics and ERK dynamics, we searched for a condition that perturbs the sustainability but not the initial amplitude of SHC translocation and noticed that in a stable cell line that overexpresses EGFR (ERBB1), derived from MCF7 cells (B1MCF7), the translocation dynamics of SHC was more transient than that in the parental

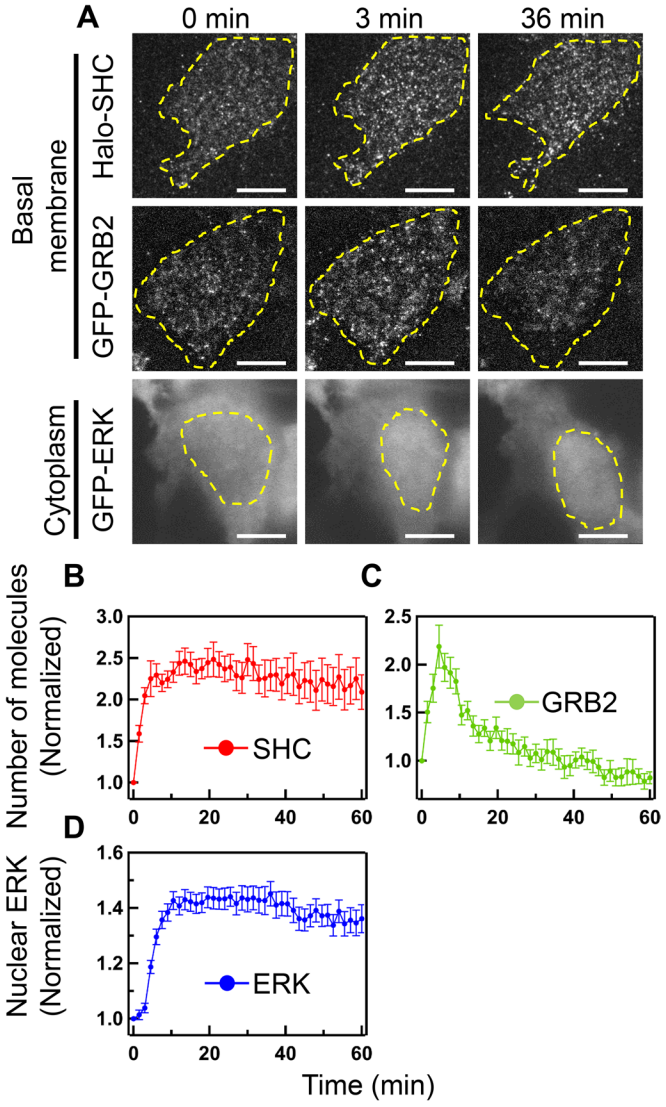

FIGURE 1: Translocation dynamics of SHC and GRB2 to the plasma membrane and of ERK to the nucleus in MCF7 cells after HRG stimulation. (A) TIRF images of Halo-SHC and GFP-GRB2 on the basal plasma membrane and epifluorescence images of GFP-ERK in MCF7 cells before (0 min) and after (3, 36 min) HRG stimulation at 25°C. Scale bar, 10 μm. (B–D) Time course analysis of Halo-SHC (B) and GFP-GRB2 (C) molecule expression on the plasma membrane and the nuclear concentration of GFP-ERK (D) in cells stimulated with 10 nM HRG at time 0. Vertical axes were normalized to the values obtained before stimulation. The mean values for 24–32 cells were plotted along with the SEs.

MCF7 cells (Figure 2, A and B). The dynamics became more sustained in B1MCF7 cells pretreated with an EGFR kinase inhibitor AG1478 (Figure 2C). On the other hand, there was no significant difference found between the translocation dynamics of GRB2 in MCF7 and in B1MCF7 cells in the presence or absence of AG1478 (Figure 2D). ERK translocation dynamics became more transient in B1MCF7 cells, and AG1478 rescued the effects of ERBB1 overexpression (Figure 2E). No association with endosomes was detectable for GRB2 or SHC, even in B1MCF7 cells after HRG stimulation (Supplemental Figure S2B). It was suggested previously that EGFR overexpression is associated with the induction of RALT/MIG6, which is a negative regulator of RAS/MAPK signaling in breast cancer (Fiorini *et al.*, 2002; Anastasi *et al.*, 2005; Nagashima *et al.*, 2009). B1MCF7 cells expressed a significantly higher level of RALT/MIG6 than the parental MCF7 cells, but no difference in ERBB2–ERBB4 expression was evident (Supplemental Figure S3, A and B). After HRG stimulation of the B1MCF7 cells, the major SHC- and GRB2-binding sites of the four ERBB receptors were persistently phosphorylated, but there were few differences with the corresponding phosphorylation levels in the parental MCF7 cells (Supplemental Figure S3C). Our findings collectively showed therefore that the translocation dynamics of SHC and ERK exhibit similar degrees of sustainability upon perturbation of EGFR receptor signaling as well as under normal conditions.

SHC-mediated PI3K activation is required for the sustained activation of ERK

To directly assess the requirements for SHC in the regulation of ERK translocation, we observed GRB2 and ERK dynamics in cells with an SHC knockdown (Figure 3A). The expression levels of SHC homologues (p46, p52, and p66) were decreased to 35–70% of the corresponding levels in the parental MCF7 cells (Supplemental Figure S5, A and B). The HRG-induced phosphorylation of the SHC- and GRB2-binding sites of some of the ERBB2–ERRB4 receptors and SHC ($pTyr^{317}$) was decreased in the SHC-knockdown MCF7 cells (Supplemental Figure S5D). The GRB2 localization at the cell surface induced by HRG stimulation was considerably suppressed in the SHC-knockdown cells, likely due to the decreased phosphorylation of the ERBBs and SHC (Figure 3D). The nuclear translocation of ERK after HRG stimulation was also affected by the SHC knockdown (Figure 3E), that is, both the peak level at the early stage (~5 min) and the sustainability of translocation were decreased. These results suggest that SHC mediates the transient membrane localization of GRB2 and sustained nuclear translocation of ERK. Further decreases in the expression of SHC (to 40% of the p52 level in the control cells) further reduced the initial peak and sustainability of SHC translocation (Supplemental Figure S5, A–C). Thus, ERK translocation was found to be affected by SHC in a dose-dependent manner.

PI3K (p85α subunit) phosphorylation at Tyr^{508}, which indicates activation, was found to be decreased in SHC-knockdown MCF7 cells (Supplemental Figure S5D), indicating that SHC positively mediates PI3K activation. We next measured the translocation dynamics of GRB2 and ERK in MCF7 cells pretreated with a kinase inhibitor for PI3K (wortmannin) to investigate whether PI3K activity is involved in the sustained activation of ERK (Figure 3B). Although the membrane localizations of SHC and GRB2 were prevented by treatment with wortmannin at a high concentration (1 μM), they were unaltered by a low concentration of this inhibitor (200 nM; Figure 3, C and D). The observed decreases in the phosphorylation levels at the GRB2-binding sites of the ERBB receptors were also marginal at best following exposure to the low concentration of wortmannin (Supplemental Figure S6, A and B). Notably, however, the nuclear translocation of ERK was found to become more transient even at the low concentration of wortmannin (Figure 3E). Almost identical results were observed in cells pretreated with 10 nM of the class I PI3K inhibitor GDC-0032 (Supplemental Figure S7, C–E).

Hence, a normal level of SHC expression is required for the full activation of PI3K and a low-level inhibition of PI3K prevents the sustained nuclear localization of ERK without affecting GRB2 translocation, suggesting that a signal transduction pathway involving PI3K functions between SHC and ERK but is independent of GRB2 (Figure 3F).

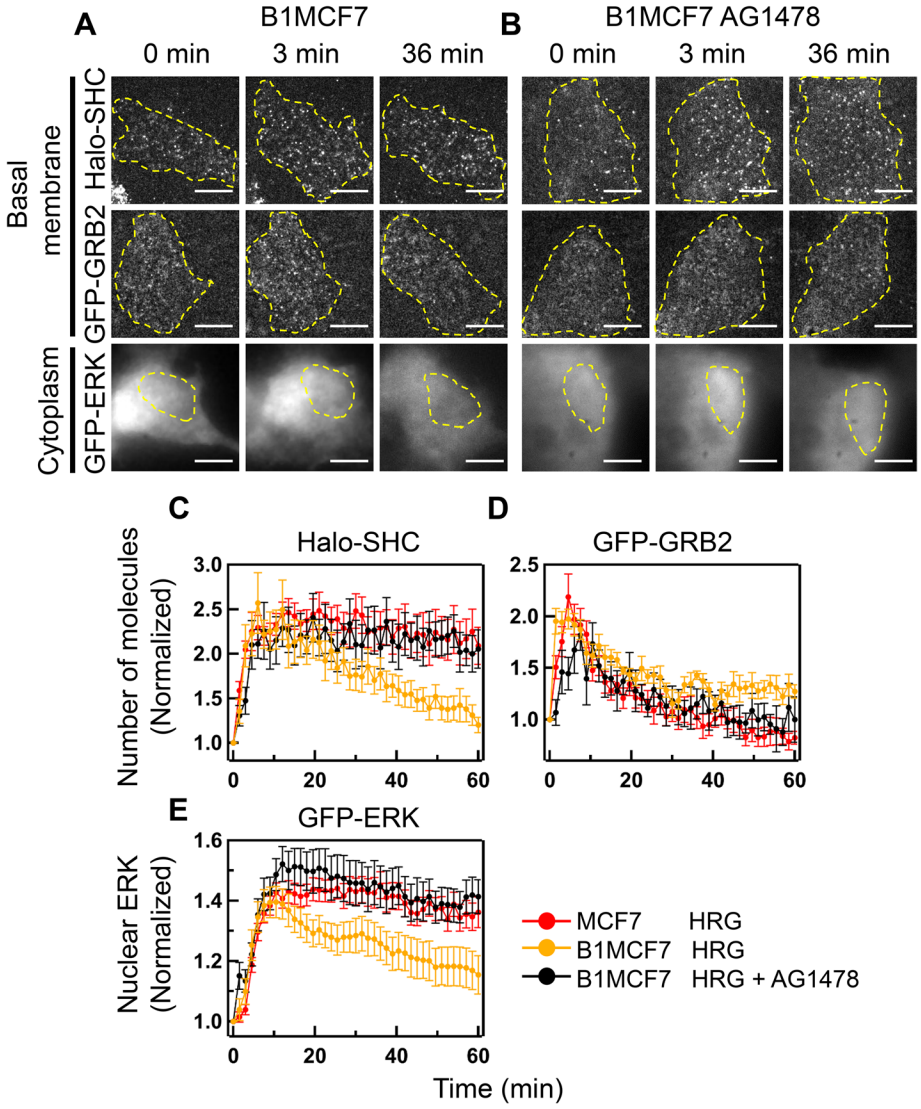

FIGURE 2: Effects of EGFR overexpression on the translocation dynamics of SHC, GRB2, and ERK. (A, B) TIRF images of Halo-SHC and GFP-GRB2 particles on the basal plasma membrane and epifluorescence images of GFP-ERK in B1MCF7 cells pretreated with (B) or without (A) 100 nM AG1478. The time periods after HRG stimulation are indicated. Scale bar, 10 μm. (C–E) Numbers of Halo-SHC (C) and GFP-GRB2 (D) molecules on the plasma membrane and nuclear concentrations of GFP-ERK (E) plotted against the time period after HRG stimulation. B1MCF7 cells without (orange) or with (black) AG1478 pretreatment were examined. Time courses for the parental MCF7 cells (shown in Figure 1) are provided for comparison (red). Values were normalized to those obtained before stimulation. The mean values for 7–32 cells were plotted with the SEs.

PI3K is involved in the sustained activation of MEK and ERK in a RAF-independent manner

PI3K was found to be translocated from the cytoplasm to the cell surface after HRG stimulation (Supplemental Figure S6C). The dynamics of the PI3K translocation were observed to be similar to those of SHC, that is, sustained in the parental MCF7 cells and more transient in the B1MCF7 cells. In the presence of AG1478, PI3K translocation in the B1MCF7 cells became sustained in a manner comparable to that in the parental cells. It is known that the production of PIP3 in the plasma membrane via PI3K activity recruits AKT from the cytoplasm to induce the phosphorylation of AKT at Thr^{308}. We confirmed that the phosphorylation at this site was decreased after treatment with both low and high concentrations of wortmannin (Supplemental Figure S6B). However, despite the distinct sustainability of the PI3K translocation in B1MCF7 cells pretreated with or without AG1478, the phosphorylation dynamics of AKT were unaffected by AG1478 (Supplemental Figure S6, C and D). This result indicated that no decrease in AKT phosphorylation is necessary to produce a transient activation of ERK.

To investigate how PI3K is involved in the sustained activation of ERK, we next measured the phosphorylation time courses for RAF, MEK1/2, and ERK1/2 (Figure 4A). The phosphorylation level at Ser^{338}, the major phosphorylation site in the active form of RAF, was slightly decreased by pretreatment with PI3K inhibitor at the low concentration (Figure 4B and Supplemental Figure S6B), but its persistence was preserved after HRG stimulation under every condition, independent of the sustainability of ERK translocation.

On the other hand, the persistence in the phosphorylation of MEK1/2 ($Ser^{217/221}$) and ERK1/2 (Thr^{202}/Tyr^{204}) after HRG stimulation, which enables their activation, was significantly reduced in B1MCF7 cells compared with the parental MCF7 cells (Figure 4B). The SHC knockdown or pretreatment with PI3K inhibitor at the low concentration reduced both the amplitude and persistence of the MEK and ERK phosphorylation in MCF7 cells. Under these conditions of a reduced sustainability of MEK and ERK phosphorylation, but with a normal sustainability of RAF phosphorylation, the translocation dynamics of SHC and ERK became more transient than seen in MCF7 cells under normal conditions (Figures 2 and 3). Based on these results, it is highly probable that SHC-regulated PI3K activity increases the amplitude of ERK activation via RAF signaling and regulates the sustainability of ERK via a signal transduction process upstream of MEK and independent of RAF.

We next examined the translocation dynamics of SHC, GRB2, and ERK in MCF7 cells pretreated with a kinase inhibitor for RAF, dabrafenib (Figure 5). In the presence of 100 nM and 10 μM dabrafenib, the HRG-induced phosphorylation of MEK was decreased to 80% and 20%, respectively, of the levels in the control cells without exposure to the inhibitor (Figure 5, A and B). The lower (100 nM) concentration of dabrafenib did not alter the translocation dynamics of SHC and GRB2. It did decrease the amplitude of ERK translocation, but, importantly, did not alter its sustainability. By comparison, the higher (10 μM) concentration of dabrafenib decreased the amplitude of SHC and GRB2 translocation and reduced both the amplitude and sustainability of ERK translocation (Figure 5, C–E). These results suggest that RAF kinase contributes to the amplitude but not the sustainability of ERK activation unless it does not affect the dynamics of GRB2 and SHC.

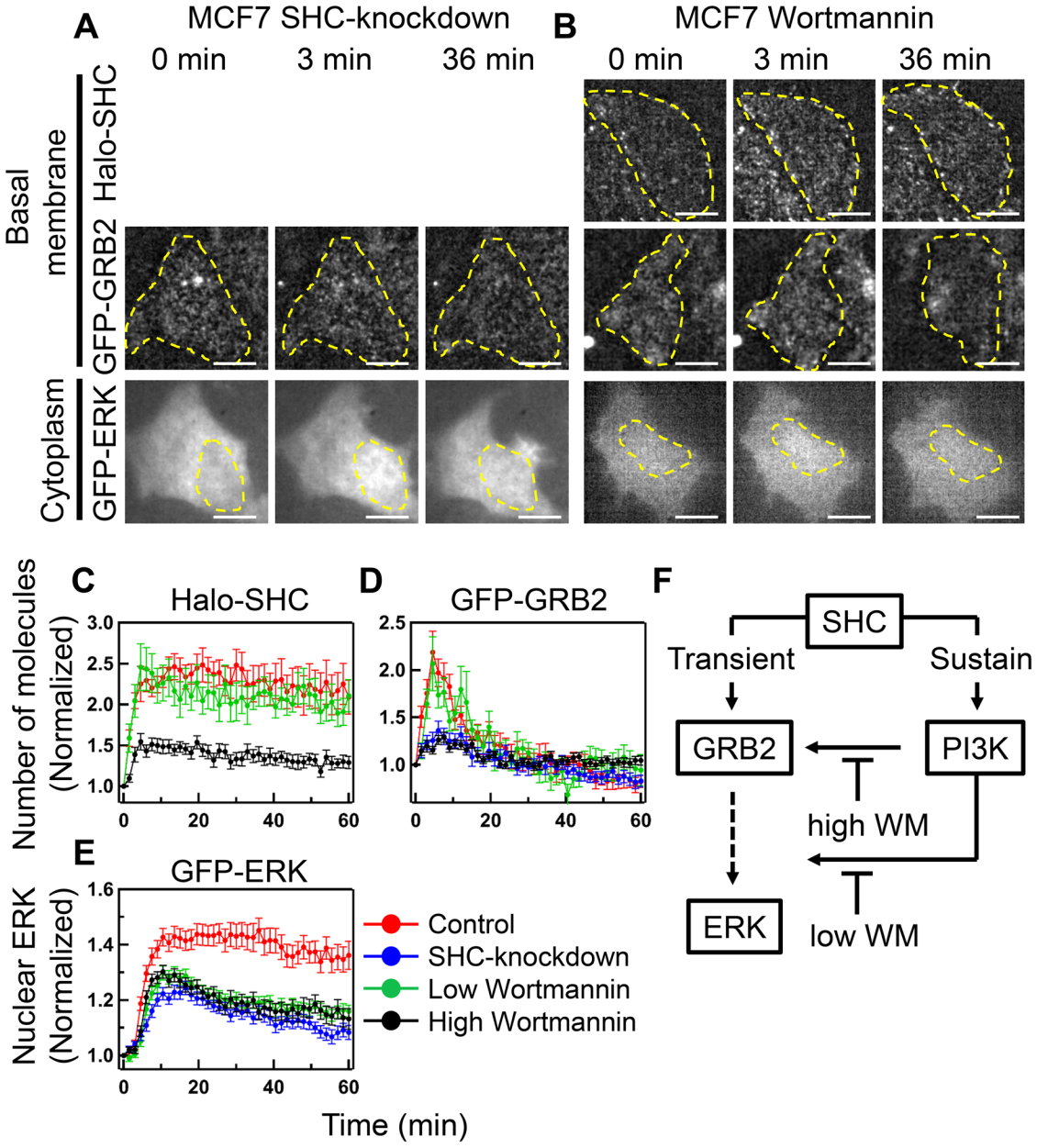

FIGURE 3: Effect of a SHC knockdown and PI3K kinase inhibition on the translocation dynamics of SHC, GRB2, and ERK. (A, B) TIRF images of Halo-SHC and GFP-GRB2 on the basal plasma membrane and epifluorescence images of GFP-ERK are shown for SHC-knockdown cells (A) and for cells pretreated with 200 nM wortmannin (B). The imaging of Halo-SHC was not applicable to the SHC-knockdown cells. Scale bar, 10 μm. (C–E) Numbers of Halo-SHC (C) and GFP-GRB2 (D) molecules on the plasma membrane and the nuclear concentrations of GFP-ERK (E) were plotted against the time period after HRG stimulation. MCF7 cells with a SHC knockdown (blue) and those pretreated with 200 nM (green) or 1 μm (black) wortmannin were examined. Time courses for the parental MCF7 cells (shown in Figure 1) are provided for comparison (red). Values were normalized to those obtained before stimulation. The mean values for 13–35 cells were plotted along with the SEs. (F) Simplified schematic representation of the possible regulatory circuit of RAS/MAPK signaling.

The translocation dynamics of SHC influences cell fate determination

We finally investigated whether the changes in the translocation dynamics of SHC and ERK observed in our experiments influenced cell fate determinations. Previous studies in MCF7 cells have reported that the transient activation of ERK leads to cell proliferation during EGF stimulation, whereas the sustained activation of ERK leads to cell differentiation during HRG stimulation (Marshall, 1995; Kao *et al.*, 2001; Nagashima *et al.*, 2007). We here quantified the proliferation and differentiation of the parental MCF7 and B1MCF7 cells (Figure 6). Although an increase in the cell density of parental MCF7 cells showed no significant difference under conditions with and without HRG in the culture medium, that of B1MCF7 cells was significantly more rapid in the presence of HRG (Figure 6A). The transient ERK activation in B1MCF7 cells stimulated with HRG promoted cell proliferation in the same manner as that stimulated with EGF.

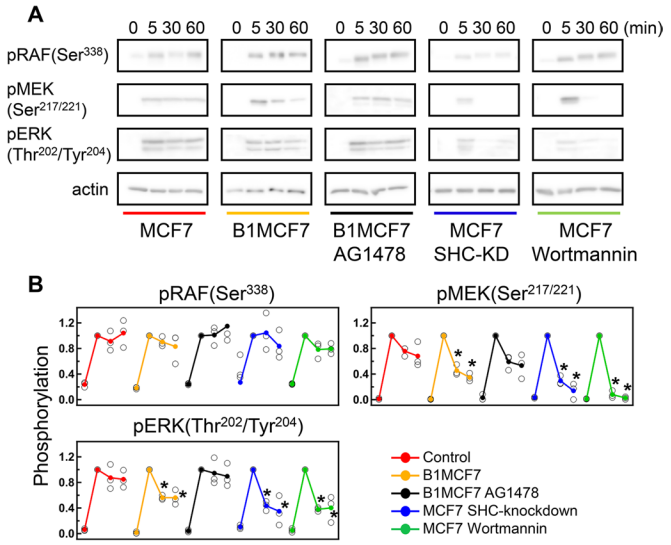

FIGURE 4: Phosphorylation dynamics of RAF, MEK1/2, and ERK1/2 after HRG stimulation. (A) Phosphorylation levels of RAF (pSer^{338}), MEK1/2 (pSer$^{217/221}$), and ERK1/2 (pThr^{202}/pTyr^{204}) under the indicated cell conditions detected by Western blotting. Wortmannin was used at a low concentration (200 nM). (B) Time courses for RAF (pSer^{338}), MEK1/2 (pSer$^{217/221}$), and ERK1/2 (pThr^{202}/pTyr^{204}) phosphorylation after HRG stimulation (0, 5, 30, 60 min from left to right). Values were normalized as described in *Materials and Methods*. The results of three independent experiments (open circle) were plotted with the mean values (closed circle). Statistical comparisons were done against the values at 5 min (*$p < 0.05$ by *t* test) to observe the sustainability under each condition.

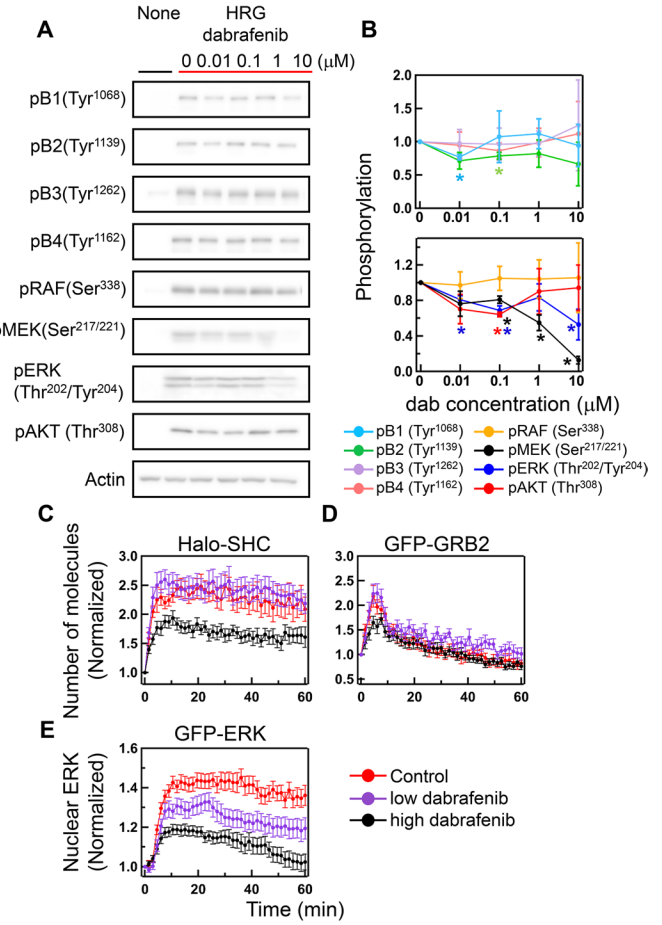

FIGURE 5: Effects of the RAF kinase inhibitor dabrafenib on RAS/MAPK and PI3K/AKT signaling in MCF7 cells. (A) Phosphorylation levels of the ERBB receptors RAF (pSer^{338}), MEK (pSer$^{217/221}$), ERK1/2 (pThr^{202}/pTyr^{204}), and AKT (Thr^{308}) under RAF kinase–inhibited conditions were detected by Western blotting. MCF7 cells were pretreated with dabrafenib at a logarithmic concentration (0–10 μM) at 37°C for 30 min before cell stimulation. (B) Phosphorylation levels of the indicated proteins. The mean values from three independent experiments were plotted along with the SD. Asterisks denote statistical significance against the values obtained for cells not exposed to dabrafenib ($p < 0.05$ by *t* test). (C–E) Numbers of Halo-SHC (C) and GFP-GRB2 (D) molecules on the plasma membrane and nuclear concentrations of GFP-ERK (E) plotted against the time period after HRG stimulation. MCF7 cells pretreated with 100 nM (purple) or 10 μM (black) dabrafenib were examined. Time courses for the parental MCF7 cells (shown in Figure 1) are provided for comparison (red). Values were normalized to those obtained before stimulation. The mean values for 17–32 cells were plotted with the SEs.

The accumulation of lipids and the formation of lipid droplets in the cytoplasm are indicators of HRG-induced differentiation in MCF7 cells (Giani *et al.*, 1998; Nagashima *et al.*, 2007). We thus quantified the lipid droplets in the parental MCF7 and B1MCF7 cells cultured with and without HRG. Consistent with the findings of previous reports, these droplets were indeed observed in the parental MCF7 cells when cultured with HRG, but not in the absence of HRG (Figure 6, B and E). Although lipid droplets were observed in a portion of the B1MCF7 cells cultured with HRG, the lipid accumulation in the cytoplasm and percentage of cells containing lipid droplets were lower than that seen in the parental MCF7 cells under the same conditions (Figure 6, C, F, and G). These results indicated that a decreased persistency in ERK activation in B1MCF7 cells attenuates HRG-induced cell differentiation. Thus, the changes in the translocation dynamics of SHC and ERK, as observed in B1MCF7 cells, could influence the determination of cell fate by switching the effects of HRG from the induction of differentiation to proliferation. The requirement of SHC activity for HRG to induce differentiation was also confirmed in MCF7 cells with the SHC knockdown (Figure 6, D, F, and G).

DISCUSSION

p52SHC (SHC) is one of the important adaptor proteins that connect receptor tyrosine kinases and downstream signaling pathways. SHC interacts with GRB2, which is also an adaptor protein that transmits signals from receptors to the RAS/MAPK and PI3K/AKT pathways. Although the SHC-mediated signaling pathway can cause a signal amplification from receptors to GRB2, qualitative differences between the signaling pathways of these two adaptor proteins have not been completely analyzed.

In our current study, we measured the translocation dynamics of SHC, GRB2, and ERK after HRG stimulation in MCF7 cells to investigate the specificity of SHC and GRB2 functions during the signaling for cell differentiation. HRG is a ligand for ERBB3 and B4, and heterodimerization between the ERBBs induces activation, that is, tyrosine phosphorylation of all four ERBBs (Miyagi *et al.*, 2020). The time courses for the translocation of SHC and GRB2 to the plasma membrane after HRG stimulation were found not to be identical, that is, SHC translocation was sustained, whereas that of GRB2 was transient (Figure 1, B and C). This result indicated that the interactions between SHC and GRB2 on the plasma membrane were not

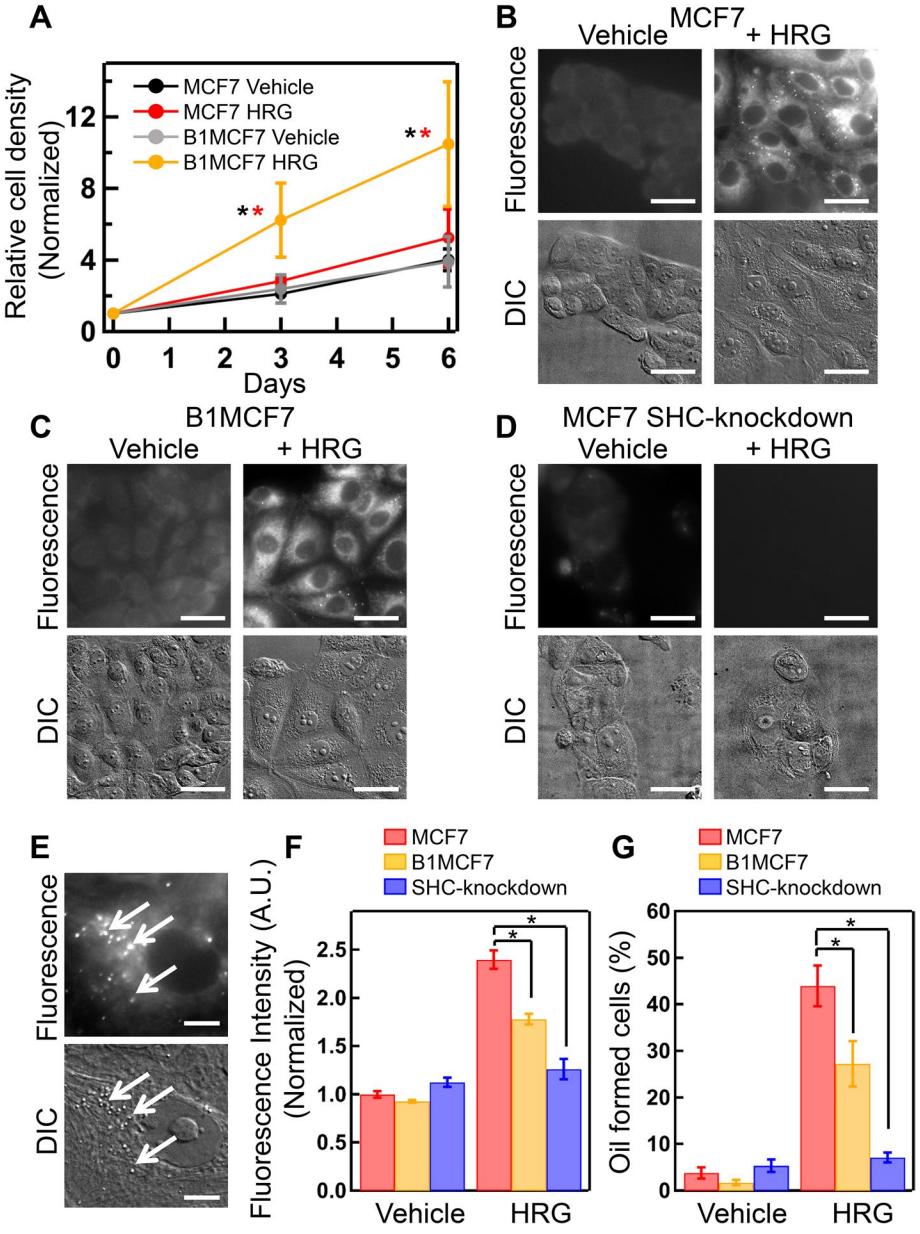

FIGURE 6: Cell proliferation and differentiation in parental MCF7 and B1MCF7 cells. (A) Proliferation time courses of MCF7 and B1MCF7 cells measured by MTT assay. Cells were cultured with vehicle or 10 nM HRG for 6 d after transfer (which was day 0). Vertical axes were normalized to the densities at day 0. The mean values for three independent experiments were plotted along with the SD. Asterisks denote statistical significance ($p < 0.05$ in *t* test) between MCF7 and B1MCF7 cells (black) and between vehicle and HRG stimulation (red). (B–D) Oil droplet formation in MCF7 (B), B1MCF7 (C), and SHC-knockdown MCF7 (D) cells, quantified using BODIPY fluorescence staining (top). Bottom panels show differential interference contrast images in the same fields of view. Scale bar, 20 μm. Cells were cultured with vehicle or 10 nM HRG for 4 d. (E) Magnified view of MCF7 cells treated with HRG. Arrows indicate BODIPY-stained oil droplets. Scale bar, 5 μm. (F, G) Fluorescence intensity in the cytoplasm (F) and percentage of cells with formed oil droplets (G) in MCF7 (red), B1MCF7 (orange), and SHC-knockdown MCF7 (blue) cultures treated with vehicle or HRG stimulation. The mean values for 111–557 cells in 11–14 views were plotted along with the SEs. Asterisks denote statistical significance ($p < 0.05$ in *t* test).

sustained after HRG stimulation. This was an unexpected finding given the conventional model in which SHC phosphorylation by the ERBBs in the plasma membrane recruits GRB2 from the cytoplasm. Although the mechanism underlying this phenomenon is not yet fully known, our current analyses suggest the involvement of EGFR (ERBB1). In the cells with EGFR overexpression (B1MCF7), the membrane translocation dynamics of SHC became more transient without affecting that of GRB2 (Figure 2, C and D).

Our present data indicate that the sustained nuclear localization and activation of ERK after HRG stimulation is positively correlated with the sustained localization of SHC to the plasma membrane but not with transient colocalization of GRB2. This suggests that the functions of SHC and GRB2 are not redundant. Moreover, our findings indicate that SHC plays critical roles in the temporal regulation of ERK activation. A previous report proposed a model of SHC-mediated RAS/MAPK signaling under EGF stimulation (Zheng *et al.*, 2013). In this model, SHC is translocated to the plasma membrane, where it interacts with phosphorylated EGFR and forms a complex with GRB2. Complexes of SHC and GRB2 on the plasma membrane are then decreased due to EGFR dephosphorylation regulated by a negative feedback loop from AKT. This model proposes similar translocation dynamics for SHC and GRB2 to the plasma membrane during EGF stimulation. Our current results have indicated, however, that these translocation dynamics of SHC and GRB2 are not necessarily similar but vary depending on the species of growth factors and cell types.

The difference between the translocation dynamics of SHC and GRB2 that we observed in our present experiments could not be explained by the differences in the phosphorylation dynamics of their binding sites on ERBB receptors (Supplemental Figure S3C). Because the endocytosis of HRG-bound receptors is reported to be slow (Wang *et al.*, 2015), most ERBB molecules probably remained on the cell surface under our experimental conditions. We could not detect either SHC or GRB2 on the endosomal membranes after HRG stimulation (Supplemental Figure S2). We recently found that phosphorylated SHC accumulated in the cytoplasm at the later stage (>30 min) of HRG signaling, where it forms complexes with GRB2 and thereby prevents it from associating with the plasma membrane (Yoshizawa *et al.*, 2021). This is a possible mechanism underlying the distinct translocation dynamics of SHC and GRB2. Another possibility in this regard is that differences in the cluster sizes of ERBB receptors cause distinct interactions with SHC and GRB2. The expression level of MIG6/RALT (ERRFI 1) was increased in our EGFR-overexpressing MCF7 cells (Supplemental Figure S3B). MIG6 is a cytoplasmic protein that interacts with the tyrosine kinase domain of EGFR, ERBB2,

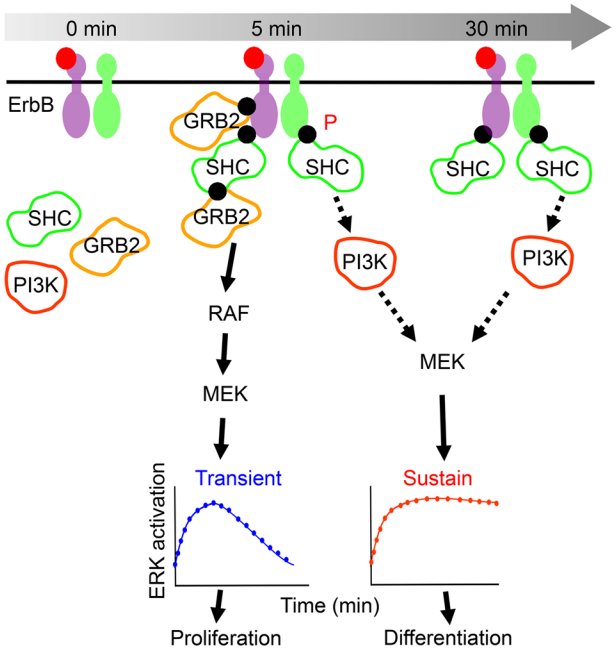

FIGURE 7: Model for the temporal regulation of ERK activation by SHC. In quiescent cells, SHC localizes in the cytoplasm. After cell stimulation, SHC is translocated to the plasma membrane and recognizes the phosphorylation sites (black circle) of ERBB receptors. The membrane localized SHC regulates the transient and sustained membrane localization of GRB2 and PI3K that transmit signals to RAF and MEK, respectively. These regulatory mechanisms are involved in the activation of ERK at the early and late stages, respectively. Dashed lines with arrows denote the pathways that have been proposed in this study.

and ERBB4 and inhibits receptor dimerization (Hackel *et al.*, 2001; Anastasi *et al.*, 2003; Zhang *et al.*, 2007; Nagashima *et al.*, 2009). The transient localization of SHC in the EGFR-overexpressing cell may indicate dimerization and/or a clustering state of ERBB receptors that distinctly regulates their affinities for adaptor proteins. It has been reported that EGFR clustering increases the affinity for GRB2 and causes the effective retention of GRB2 on the plasma membrane (Jadwin *et al.*, 2016; Hiroshima *et al.*, 2018).

Our present results indicate that SHC regulates both the initial amplitude and sustainability of ERK activation in MCF7 cells stimulated with HRG. The SHC-GRB2/SOS-RAS pathway was found to be principally responsible for the initial amplitude, while the SHC-PI3K pathway was observed to be important for the sustainability of ERK activation (Figure 7). The sustainability also depended on the initial amplitude, that is, when the initial amplitude was insufficient, ERK activation could not be prolonged. In other words, GRB2-RAF signaling is the initiator of ERK activation and SHC-PI3K signaling is a modulator of its dynamics of ERK activation. Such differential roles between GRB2 and SHC may underlie previous findings that a mouse knockout of GRB2 (Cheng *et al.*, 1998) is early embryonic lethal, whereas a knockout of SHC did not produce any significant phenotypes other than defects in the cardiovascular system (Lai and Pawson, 2000).

HRG is a ligand of ERBB3, which is known to have the highest affinity for PI3K among the ERBB subtypes (Falls, 2003; Schulze *et al.*, 2005; Dey *et al.*, 2015). Notably, however, the pathways connecting SHC to PI3K that are indicated by our current observations remain unknown. Although several studies have suggested that a complex formation occurs between SHC and PI3K via the 14-3-3 protein (Ursini-Siegel *et al.*, 2012; Suen *et al.*, 2018), it is not certain whether this underpinned any of our present findings. PI3K is one of the effectors of RAS (Vivanco and Sawyers, 2002; Castellano and Downward, 2011). However, we found in our previous study under the same experimental conditions as used here that the translocation of RAF to the plasma membrane, which reflects the activation dynamics of RAS, was transient (Yoshizawa *et al.*, 2021). Hence, the RAS-PI3K pathway is less likely to induce a sustained activation of PI3K (Supplemental Figure S6C). A positive feedback loop involving GRB2 and PI3K has been reported previously, that is, whereby GRB2 enhances PI3K activation via GRB2-associated binder 1 (GAB1) and extends the duration of RAS/MAPK signaling (Kiyatkin *et al.*, 2006; Aasrum *et al.*, 2013). These same reports have suggested that the GAB1-PI3K interaction positively regulates RAS/MAPK signaling by increasing the membrane recruitment of the GRB2-SOS complexes that activate RAS and of SHP2 that negatively regulates RASGAP signaling. In our current study, we found that an SHC knockdown or strong inhibition of PI3K reduced the membrane localization of GRB2 and caused the translocation dynamics of ERK to become more transient (Figure 3, D and E). Our current results are thus consistent with the idea that the GAB1-PI3K positive feedback loop increases the amplitude of ERK activation.

It was notable from our present analyses also that a low concentration of the PI3K inhibitors caused the ERK translocation dynamics to be more transient, with no effect on GRB2 dynamics (Figure 3, D and E; Supplemental Figure S7, D and E). The low concentration of wortmannin reduced the persistence of MEK, whereas the sustainability in RAF phosphorylation was not significantly changed (Figure 4B). EGFR overexpression (B1MCF7 cells) and the SHC knockdown produced effects on RAF, MEK, and ERK that were similar to the impact of low doses of PI3K inhibitors (Figure 4B). These results indicated that in addition to the GRB2/RAF-dependent pathway mentioned above, another signaling pathway operates in a RAF-independent manner by which SHC regulates ERK activation through PI3K (Figure 7). The GRB2-dependent pathway regulates the amplitude of the initial response of ERK via RAF activation, whereas our putative GRB2- and RAF-independent pathway appears to regulate the sustainability of ERK. A sufficiently high initial activation of ERK is required for the latter pathway to function.

The GRB2- and RAF-independent pathway from PI3K to MEK suggested by our present study has not previously been described, to our knowledge, as part of the ERBB system for regulating the sustainability of ERK signaling. The results of our current proliferation and differentiation assays (Figure 6) support the idea that the PI3K-MEK signaling regulated by SHC is a significant pathway for cell fate determination. PAK and PDK1 are known protein kinases that function downstream of PI3K and are involved in RAS/MAPK signaling (Rodriguez-Viciana *et al.*, 1997; Toker and Cantley, 1997; Vanhaesebroeck *et al.*, 1997). PAK phosphorylates RAF (Ser^{338}) and MEK1 (Ser^{298}) to increase the phosphorylation ($Ser^{218/222}$) and activity of MEK1 (Zang *et al.*, 2002; Park *et al.*, 2007; Eblen, 2018). PDK1 phosphorylates AKT (Thr^{308}) and is involved in the phosphorylation and activation of many other protein kinases (Belham *et al.*, 1999; Vanhaesebroeck and Alessi, 2000). It has also been reported that PDK1 directly phosphorylates MEK1/2 ($Ser^{222/226}$) without affecting the activity of RAF (Sato *et al.*, 2004). It is probable that the PI3K activity regulated by SHC activates PAK and/or PDK1 to induce the sustained phosphorylation of MEK and ERK during HRG stimulation. However, it is difficult to analyze each specific phosphorylation reaction of these kinases in living cells because they are involved in the phosphorylation of multiple proteins in the ERBB-RAS-MAPK signaling pathway. Future research will hopefully uncover more of the detailed dynamics of this phosphorylation reaction network.

MATERIALS AND METHODS

Request a protocol through *Bio-protocol*.

Plasmids and construction

CMV-p52SHC and GFP-p52SHC plasmids were kindly provided by Kenichi Sato at Kyoto Sangyo University. The pmEGFP-C2 (BD Biosciences, Franklin Lakes, NJ) transfer vector harboring a monomeric mutation of GFP was constructed through a direct point mutation of A206K in the pmEGFP-C2 vector, as described previously (Hibino *et al.*, 2011). To construct the mEGFP-GRB2 (GFP-GRB2) and mEGFP-ERK2 (GFP-ERK) transfer vectors, CMV-GRB2 (Morimatsu *et al.*, 2007) and CMV-ERK (Takahashi *et al.*, 2012) fragments were subcloned into the *Bgl*II-*Xho*I and *Bgl*II-*Bam*HI sites of the pmEGFP-C2 vector, respectively. The Halo7-C1 vector was constructed by exchanging mEGFP for Halo7 (pFN19 HhaloTag T7 SP6 Flexi vector; Promega, Madison, WI) in the EGFP-C1 vector (Takara Bio, Shiga, Japan). p85α was kindly provided by Pablo Rodriguez-Viciana at the UCL Cancer Institute. To construct the Halo7-p52SHC (Halo-SHC) and Halo7-p85α (Halo-p85α) transfer vectors, CMV-p52SHC and p85α inserts were subcloned into the *Sac*I-*Kpn*I and *Eco*RI-*Bam*HI sites of the Halo7-C1 vector, respectively.

Cell culture and transfection

MCF7 cells and EGFR-overexpressing MCF7 cells (B1MCF7) (Nagashima *et al.*, 2015) were cultured in DMEM (Wako Pure Chemical Industries, Osaka, Japan) supplemented with 10% fetal bovine serum (FBS) in a 5% CO_2 incubator at 37°C. Cells were transfected with expression vectors as described previously (Nakamura *et al.*, 2016) and then serum starved in MEM (Nissui, Tokyo, Japan) containing 1.5 mg/ml $NaHCO_3$, 0.3 mg/ml L-glutamine, 15 mM HEPES (pH 7.4; Nacalai Tesque, Kyoto, Japan), and 0.1% fatty acid–free bovine serum albumin (BSA) (Wako Pure Chemical Industry) in a CO_2 incubator for 24 h. To detect Halo-p52SHC expression, the cells were labeled with 100 nM HaloTag tetramethylrhodamine (TMR; Promega) in culture medium at 37°C for 15 min, as described previously (Nakamura *et al.*, 2016), and washed repeatedly with Hanks' Balanced Salt Solution (HBSS) (Sigma-Aldrich, St. Louis, MO). The medium was then replaced with MEM containing 5 mM HEPES (pH 7.4) and 0.1% BSA. For the inducible knockdown of SHC, we used ON-TARGETplus Human SHC1 siRNA (Dharmacon, Lafayette, CO).

Fluorescence imaging

The localizations of fluorescently labeled Halo-SHC, GFP-GRB2, and GFP-ERK were observed using a confocal laser scanning microscope (TCS SP2; Leica, Wetzlar, Germany) equipped with a 63×, NA 1.20 objective lens (HCX PL Apo; Leica) at 25°C, with excitation at 488 and 543 nm and detection at 510–600 and 560–650 nm. Single molecules of fluorescently labeled Halo-SHC and GFP-GRB2 expressed at the plasma membrane and the intracellular distribution of GFP-ERK were observed using TIRFM based on an inverted microscope (IX83; Olympus, Tokyo, Japan) equipped with a 60×, NA 1.49 oil immersion objective (ApoN; Olympus) at 25°C, as described previously (Yoshizawa *et al.*, 2017) with some modifications. Briefly, for the selective fluorescence excitation of GFP and TMR, OPSL lasers (Sapphire 488 LP and Sapphire 561 LP; Coherent, Santa Clara, CA) and a ZT 488/561 rpc dichroic mirror (Chroma Technology, Bellows Falls, VT) were used. To acquire emission signals for the 505–530 nm (GFP) and 560–650 nm (TMR) wavelengths simultaneously, a WVIEW GEMINI-2C (Hamamatsu Photonics K. K., Shizuoka, Japan) was used equipped with a T560lpxr dichroic mirror (Chroma Technology) and two emission filters, that is, FF01-514/30-25 514 nm (Semrock, Rochester, NY) for GFP and FF01-605/64-25 605/64 nm BrightLine single-band bandpass filter (Laser 2000, Cambridgeshire, UK) for TMR, respectively. Fluorescence images were acquired using two ORCA-Flash 4.0 V3 Digital CMOS cameras (Hamamatsu Photonics K. K.) at 20 fps.

Under the microscope at 25°C, the cells were stimulated with a final concentration of 10 nM recombinant human NRG1-β1/HRG1-β1 EGF domain (HRG; R&D Systems, Minneapolis, MN). For the inhibition of the kinase activities of EGFR and RAF, cells were pretreated with 100 nM AG1478 and 100 nM or 10 μM dabrafenib (ChemScene, Monmouth Junction, NJ) for 30 min before stimulation, respectively. For the inhibition of PI3K kinase activity, cells were pretreated with 200 nM or 1 μM wortmannin (Wako Pure Chemical Industries) for 30 min or 10 nM GDC-0032 (Cayman Chemical, Ann Arbor, MI) for 2 h before stimulation. The translocation dynamics of Halo-SHC and GFP-GRB2 at the plasma membrane and GFP-ERK from the cytoplasm to the nucleus, respectively, were observed on the basal plasma membrane and in the cytoplasm of MCF7 cells for 60 min after HRG stimulation using 1.5 min time-lapse imaging, alternatively changing the illumination mode between TIR and epi (Yoshizawa *et al.*, 2017). Fluorescent particles of Halo-SHC and GFP-GRB2 on the basal plasma membrane in each frame were detected using G-Count Software (G-Angstrom, Miyagi, Japan). The relative numbers of these molecules on the plasma membrane were calculated by multiplying the number of fluorescent particles by their fluorescence intensity. To quantify the relative nuclear concentration of GFP-ERK, the average fluorescence intensity of GFP-ERK per area in the nucleus was calculated. The amplitude dynamics of Halo-SHC, GFP-GRB2, and GFP-ERK were normalized with the values obtained before stimulation in each cell.

Cell proliferation assay

To analyze the proliferation of MCF7 and B1MCF7 cells, the CytoSelectTM MTT Cell Proliferation Assay (Cell Biolabs, San Diego, CA) was used. After 0–6 d of culture on a 96-well plate, MTT reagent (10 μl) was added to each well and the plates were incubated in a CO_2 incubator. After 3.5 h, the medium was replaced with 100 μl detergent solution and the plates were incubated at room temperature for 2 h. The absorbance at 540 nm was then measured using a microplate reader (Epoch2; Bio-Tek Instruments, Winooski, VT).

Quantitative analysis of cell differentiation

Oil droplet formation was assayed using the Adipocyte Fluorescent Staining Kit (Primary Cell, Hokkaido, Japan). Cells were cultured on an eight-well Lab-Tek Chambered Coverglass (Nunc, Rochester, NY). After 4-d culture in DMEM supplemented with 10% FBS with or without 10 nM HRG, the cells were fixed with phosphate-buffered saline (PBS) containing 3% paraformaldehyde (Wako Pure Chemical Industries) at room temperature for 10 min, washed repeatedly with PBS, and then incubated with BODIPY at room temperature for 30 min. After further repeat washes with PBS, cells were mounted with a mounting agent, incubated at 4°C for 30 min, and observed under an inverted microscope (IX81; Olympus) equipped with a 60×, NA 1.45 oil immersion objective lens (Plan Apo; Olympus). For the detection of BODIPY fluorescence (excitation peak 498 nm, emission peak 503 nm) a U-MNIBA2 filter set (Olympus) was used. Images were acquired using an ORCA-Flash 4.0 V2 Digital CMOS camera with 0.5 s exposure.

Western blotting

For Western blotting analysis, primary antibodies against the following proteins were used to quantify the expression level: ERBB1

(sc-03; Santa Cruz Biotechnology, Dallas, TX), ERBB2 (2165; Cell Signaling Technology [CST], Danvers, MA), ERBB3 (sc-285; Santa Cruz Biotechnology), ERBB4 (sc-283; Santa Cruz Biotechnology), MIG6/ERRFI1 (11630-1-AP; Proteintech, Rosemont, IL), SHC (06-203; Millipore, Burlington, MA), GRB2 (610111; BD Biosciences), and β-actin (A5441; Sigma-Aldrich). The following primary antibodies were used to quantify the phosphorylation level of each protein: anti-pERBB1 (pTyr^{1068}; 3777; CST), anti-pERBB1 (pTyr^{1173}; 4407; CST), anti-pERBB2 (pTyr^{1139}; ab53290; Abcam, Cambridge, UK), anti-pERBB2 (pTyr$^{1221/2}$; 2243; CST), anti-pERBB3 (pTyr^{1262}; AF5817; R&D Systems), anti-pERBB3 (pTyr^{1328}; ab131444; Abcam), anti-pERBB4 (pTyr^{1162}; ab68478; Abcam), anti-pERBB4 (pTyr^{1284}; 4757; CST), anti-pSHC (pTyr^{317}; 2431; CST), anti-pRAF (pSer^{338}; 05-538; Millipore), anti-pMEK1/2 (pSer$^{217/221}$; 9121; CST), anti-pERK1/2 (pThr^{202}/pTyr^{204}; 9106; CST), anti–p-PI3K p85α (pTyr^{508}; sc-12929; Santa Cruz Biotechnology), and anti-pAKT (pThr308; 9275; CST).

Two normalization steps were used to enable an accurate comparison of the phosphorylation levels from the immunoblotting data. First, all experimental data were normalized to the staining intensities of β-actin to observe the relative amounts of phosphorylated proteins per cell. Second, time series data obtained from the same experiment were normalized using the maximum intensities observed at 5 min.

ACKNOWLEDGMENTS

R.Y. was supported by a Grant-in-Aid for JSPS (Japan Society for the Promotion of Science) Fellows. Y.S. was supported by MEXT Japan with Grants-in-Aid for Scientific Research (17H06021, 19H05647) and by JST (Japan Science and Technology Agency) CREST (JPMJCR1912). We thank Hiromi Sato for technical assistance and Kenichi Sato and Pablo Rodriguez-Viciana for providing expression vectors.

REFERENCES

Aasrum M, Odegard J, Sandnes D, Christoffersen T (2013). The involvement of the docking protein Gab1 in mitogenic signalling induced by EGF and HGF in rat hepatocytes. Biochim Biophys Acta 1833, 3286–3294.

Anastasi S, Fiorentino L, Fiorini M, Fraioli R, Sala G, Castellani L, Alema S, Alimandi M, Segatto O (2003). Feedback inhibition by RALT controls signal output by the ErbB network. Oncogene 22, 4221–4234.

Anastasi S, Sala G, Huiping C, Caprini E, Russo G, Iacovelli S, Lucini F, Ingvarsson S, Segatto O (2005). Loss of RALT/MIG-6 expression in ERBB2-amplified breast carcinomas enhances ErbB-2 oncogenic potency and favors resistance to herceptin. Oncogene 24, 4540–4548.

Avraham R, Yarden Y (2011). Feedback regulation of EGFR signalling: decision making by early and delayed loops. Nat Rev Mol Cell Biol 12, 104–117.

Belham C, Wu S, Avruch J (1999). Intracellular signalling: PDK1—a kinase at the hub of things. Curr Biol 9, R93–R96.

Birtwistle MR, Hatakeyama M, Yumoto N, Ogunnaike BA, Hoek JB, Kholodenko BN (2007). Ligand-dependent responses of the ErbB signaling network: experimental and modeling analyses. Mol Syst Biol 3, 144.

Bisson N, James DA, Ivosev G, Tate SA, Bonner R, Taylor L, Pawson T (2011). Selected reaction monitoring mass spectrometry reveals the dynamics of signaling through the GRB2 adaptor. Nat Biotechnol 29, 653–658.

Bouchard C, Marquardt J, Bras A, Medema RH, Eilers M (2004). Myc-induced proliferation and transformation require Akt-mediated phosphorylation of FoxO proteins. EMBO J 23, 2830–2840.

Brunet A, Roux D, Lenormand P, Dowd S, Keyse S, Pouyssegur J (1999). Nuclear translocation of p42/p44 mitogen-activated protein kinase is required for growth factor-induced gene expression and cell cycle entry. EMBO J 18, 664–674.

Castellano E, Downward J (2011). RAS interaction with PI3K: more than just another effector pathway. Genes Cancer 2, 261–274.

Caunt CJ, McArdle CA (2012). ERK phosphorylation and nuclear accumulation: insights from single-cell imaging. Biochem Soc Trans 40, 224–229.

Cheng AM, Saxton TM, Sakai R, Kulkarni S, Mbamalu G, Vogel W, Tortorice CG, Cardiff RD, Cross JC, Muller WJ, Pawson T (1998). Mammalian Grb2 regulates multiple steps in embryonic development and malignant transformation. Cell 95, 793–803.

Davol PA, Bagdasaryan R, Elfenbein GJ, Maizel AL, Frackelton AR Jr (2003). Shc proteins are strong, independent prognostic markers for both node-negative and node-positive primary breast cancer. Cancer Res 63, 6772–6783.

Dey N, Williams C, Leyland-Jones B, De P (2015). A critical role for HER3 in HER2-amplified and non-amplified breast cancers: function of a kinase-dead RTK. Am J Transl Res 7, 733–750.

Eblen ST (2018). Extracellular-regulated kinases: signaling from Ras to ERK substrates to control biological outcomes. Adv Cancer Res 138, 99–142.

Egan SE, Giddings BW, Brooks MW, Buday L, Sizeland AM, Weinberg RA (1993). Association of Sos Ras exchange protein with Grb2 is implicated in tyrosine kinase signal transduction and transformation. Nature 363, 45–51.

Falls DL (2003). Neuregulins: functions, forms, and signaling strategies. Exp Cell Res 284, 14–30.

Fiorini M, Ballaro C, Sala G, Falcone G, Alema S, Segatto O (2002). Expression of RALT, a feedback inhibitor of ErbB receptors, is subjected to an integrated transcriptional and post-translational control. Oncogene 21, 6530–6539.

Giani C, Casalini P, Pupa SM, De Vecchi R, Ardini E, Colnaghi MI, Giordano A, Menard S (1998). Increased expression of c-erbB-2 in hormone-dependent breast cancer cells inhibits cell growth and induces differentiation. Oncogene 17, 425–432.

Gu H, Maeda H, Moon JJ, Lord JD, Yoakim M, Nelson BH, Neel BG (2000). New role for Shc in activation of the phosphatidylinositol 3-kinase/Akt pathway. Mol Cell Biol 20, 7109–7120.

Hackel PO, Gishizky M, Ullrich A (2001). Mig-6 is a negative regulator of the epidermal growth factor receptor signal. Biol Chem 382, 1649–1662.

Hibino K, Shibata T, Yanagida T, Sako Y (2011). Activation kinetics of RAF protein in the ternary complex of RAF, RAS-GTP, and kinase on the plasma membrane of living cells: single-molecule imaging analysis. J Biol Chem 286, 36460–36468.

Hiroshima M, Pack CG, Kaizu K, Takahashi K, Ueda M, Sako Y (2018). Transient acceleration of epidermal growth factor receptor dynamics produces higher-order signaling clusters. J Mol Biol 430, 1386–1401.

Jadwin JA, Oh D, Curran TG, Ogiue-Ikeda M, Jia L, White FM, Machida K, Yu J, Mayer BJ (2016). Time-resolved multimodal analysis of Src homology 2 (SH2) domain binding in signaling by receptor tyrosine kinases. eLife 5, e11835.

Kao S, Jaiswal RK, Kolch W, Landreth GE (2001). Identification of the mechanisms regulating the differential activation of the MAPK cascade by epidermal growth factor and nerve growth factor in PC12 cells. J Biol Chem 276, 18169–18177.

Kiyatkin A, Aksamitiene E, Markevich NI, Borisov NM, Hoek JB, Kholodenko BN (2006). Scaffolding protein Grb2-associated binder 1 sustains epidermal growth factor-induced mitogenic and survival signaling by multiple positive feedback loops. J Biol Chem 281, 19925–19938.

Lai KM, Pawson T (2000). The ShcA phosphotyrosine docking protein sensitizes cardiovascular signaling in the mouse embryo. Genes Dev 14, 1132–1145.

Marshall CJ (1995). Specificity of receptor tyrosine kinase signaling: transient versus sustained extracellular signal-regulated kinase activation. Cell 80, 179–185.

Mendoza MC, Er EE, Blenis J (2011). The Ras-ERK and PI3K-mTOR pathways: cross-talk and compensation. Trends Biochem Sci 36, 320–328.

Miyagi H, Hiroshima M, Sako Y (2020). Cell-to-cell diversification in ERBB-RAS-MAPK signal transduction that produces cell-type specific growth factor responses. Biosystems 199, 104293.

Morimatsu M, Takagi H, Ota KG, Iwamoto R, Yanagida T, Sako Y (2007). Multiple-state reactions between the epidermal growth factor receptor and Grb2 as observed by using single-molecule analysis. Proc Natl Acad Sci USA 104, 18013–18018.

Nagashima T, Inoue N, Yumoto N, Saeki Y, Magi S, Volinsky N, Sorkin A, Kholodenko BN, Okada-Hatakeyama M (2015). Feedforward regulation of mRNA stability by prolonged extracellular signal-regulated kinase activity. FEBS J 282, 613–629.

Nagashima T, Shimodaira H, Ide K, Nakakuki T, Tani Y, Takahashi K, Yumoto N, Hatakeyama M (2007). Quantitative transcriptional control of ErbB receptor signaling undergoes graded to biphasic response for cell differentiation. J Biol Chem 282, 4045–4056.

Nagashima T, Ushikoshi-Nakayama R, Suenaga A, Ide K, Yumoto N, Naruo Y, Takahashi K, Saeki Y, Taiji M, Tanaka H, *et al.* (2009). Mutation of epidermal growth factor receptor is associated with MIG6 expression. FEBS J 276, 5239–5251.
Nakakuki T, Yumoto N, Naka T, Shirouzu M, Yokoyama S, Hatakeyama M (2008). Topological analysis of MAPK cascade for kinetic ErbB signaling. PLoS One 3, e1782.
Nakamura Y, Hibino K, Yanagida T, Sako Y (2016). Switching of the positive feedback for RAS activation by a concerted function of SOS membrane association domains. Biophys Physicobiol 13, 1–11.
Nepstad I, Hatfield KJ, Grønningsæter IS, Reikvam H (2020). The PI3K-Akt-mTOR signaling pathway in human acute myeloid leukemia (AML) cells. Int J Mol Sci 21, 2907.
Oku S, van der Meulen T, Copp J, Glenn G, van der Geer P (2012). Engineering NGF receptors to bind Grb2 directly uncovers differences in signaling ability between Grb2- and ShcA-binding sites. FEBS Lett 586, 3658–3664.
Park ER, Eblen ST, Catling AD (2007). MEK1 activation by PAK: a novel mechanism. Cell Signal 19, 1488–1496.
Pawson T (2007). Dynamic control of signaling by modular adaptor proteins. Curr Opin Cell Biol 19, 112–116.
Pelicci G, Lanfrancone L, Grignani F, McGlade J, Cavallo F, Forni G, Nicoletti I, Grignani F, Pawson T, Pelicci PG (1992). A novel transforming protein (SHC) with an SH2 domain is implicated in mitogenic signal transduction. Cell 70, 93–104.
Ravichandran KS (2001). Signaling via Shc family adapter proteins. Oncogene 20, 6322–6330.
Rodriguez-Viciana P, Warne PH, Khwaja A, Marte BM, Pappin D, Das P, Waterfield MD, Ridley A, Downward J (1997). Role of phosphoinositide 3-OH kinase in cell transformation and control of the actin cytoskeleton by Ras. Cell 89, 457–467.
Santos SD, Verveer PJ, Bastiaens PI (2007). Growth factor-induced MAPK network topology shapes Erk response determining PC-12 cell fate. Nat Cell Biol 9, 324–330.
Sasagawa S, Ozaki Y, Fujita K, Kuroda S (2005). Prediction and validation of the distinct dynamics of transient and sustained ERK activation. Nat Cell Biol 7, 365–373.
Sato S, Fujita N, Tsuruo T (2004). Involvement of 3-phosphoinositide-dependent protein kinase-1 in the MEK/MAPK signal transduction pathway. J Biol Chem 279, 33759–33767.
Saucier C, Khoury H, Lai KM, Peschard P, Dankort D, Naujokas MA, Holash J, Yancopoulos GD, Muller WJ, Pawson T, Park M (2004). The Shc adaptor protein is critical for VEGF induction by Met/HGF and ErbB2 receptors and for early onset of tumor angiogenesis. Proc Natl Acad Sci USA 101, 2345–2350.
Saucier C, Papavasiliou V, Palazzo A, Naujokas MA, Kremer R, Park M (2002). Use of signal specific receptor tyrosine kinase oncoproteins reveals that pathways downstream from Grb2 or Shc are sufficient for cell transformation and metastasis. Oncogene 21, 1800–1811.
Schulze WX, Deng L, Mann M (2005). Phosphotyrosine interactome of the ErbB-receptor kinase family. Mol Syst Biol 1, 2005.0008.
Songyang Z, Shoelson SE, McGlade J, Olivier P, Pawson T, Bustelo XR, Barbacid M, Sabe H, Hanafusa H, Yi T, *et al.* (1994). Specific motifs recognized by the SH2 domains of Csk, 3BP2, fps/fes, GRB-2, HCP, SHC, Syk, and Vav. Mol Cell Biol 14, 2777–2785.
Sparks AB, Rider JE, Hoffman NG, Fowlkes DM, Quillam LA, Kay BK (1996). Distinct ligand preferences of Src homology 3 domains from Src, Yes, Abl, cortactin, p53bp2, PLCgamma, Crk, and Grb2. Proc Natl Acad Sci USA 93, 1540–1544.
Suen KM, Lin CC, Seiler C, George R, Poncet-Montange G, Biter AB, Ahmed Z, Arold ST, Ladbury JE (2018). Phosphorylation of threonine residues on Shc promotes ligand binding and mediates crosstalk between MAPK and Akt pathways in breast cancer cells. Int J Biochem Cell Biol 94, 89–97.
Takahashi M, Shibata T, Yanagida T, Sako Y (2012). A protein switch with tunable steepness reconstructed in Escherichia coli cells with eukaryotic signaling proteins. Biochem Biophys Res Commun 421, 731–735.
Toker A, Cantley LC (1997). Signalling through the lipid products of phosphoinositide-3-OH kinase. Nature 387, 673–676.
Ursini-Siegel J, Hardy WR, Zheng Y, Ling C, Zuo D, Zhang C, Podmore L, Pawson T, Muller WJ (2012). The ShcA SH2 domain engages a 14-3-3/PI3′K signaling complex and promotes breast cancer cell survival. Oncogene 31, 5038–5044.
Vanhaesebroeck B, Alessi DR (2000). The PI3K-PDK1 connection: more than just a road to PKB. Biochem J 346(Pt 3), 561–576.
Vanhaesebroeck B, Leevers SJ, Panayotou G, Waterfield MD (1997). Phosphoinositide 3-kinases: a conserved family of signal transducers. Trends Biochem Sci 22, 267–272.
Vivanco I, Sawyers CL (2002). The phosphatidylinositol 3-kinase AKT pathway in human cancer. Nat Rev Cancer 2, 489–501.
Wang Q, Chen X, Wang Z (2015). Dimerization drives EGFR endocytosis through two sets of compatible endocytic codes. J Cell Sci 128, 935–950.
Yoshizawa R, Umeki N, Yamamoto A, Murata M, Sako Y (2021). Biphasic spatiotemporal regulation of GRB2 dynamics by p52SHC for transient RAS activation. Biophys Physicobiol 18, 1–12.
Yoshizawa R, Umeki N, Yanagawa M, Murata M, Sako Y (2017). Single-molecule fluorescence imaging of RalGDS on cell surfaces during signal transduction from Ras to Ral. Biophys Physicobiol 14, 75–84.
Zang M, Hayne C, Luo Z (2002). Interaction between active Pak1 and Raf-1 is necessary for phosphorylation and activation of Raf-1. J Biol Chem 277, 4395–4405.
Zhang X, Pickin KA, Bose R, Jura N, Cole PA, Kuriyan J (2007). Inhibition of the EGF receptor by binding of MIG6 to an activating kinase domain interface. Nature 450, 741–744.
Zheng Y, Zhang C, Croucher DR, Soliman MA, St-Denis N, Pasculescu A, Taylor L, Tate SA, Hardy WR, Colwill K, *et al.* (2013). Temporal regulation of EGF signalling networks by the scaffold protein Shc1. Nature 499, 166–171.